0026-895X/05/6806-1669–1677$20.00
MOLECULAR PHARMACOLOGY
Copyright © 2005 The American Society for Pharmacology and Experimental Therapeutics
Mol Pharmacol 68:1669–1677, 2005

Vol. 68, No. 6
15446/3062709
Printed in U.S.A.

Mutations of a Conserved Lysine Residue in the N-Terminal Domain of $\alpha 7$ Nicotinic Receptors Affect Gating and Binding of Nicotinic Agonists

Manuel Criado, José Mulet, José A. Bernal, Susana Gerber, Salvador Sala, and Francisco Sala

Instituto de Neurociencias de Alicante, Universidad Miguel Hernández-Consejo Superior de Investigaciones Cientificas, Alicante, Spain

Received June 1, 2005; accepted August 29, 2005

ABSTRACT

Activation of nicotinic acetylcholine receptors is initiated by binding of agonists, and as a consequence, specific domains transmit the chemical signal to the channel gate through a sequence of conformational changes. Recent high-resolution structural data from a snail acetylcholine binding protein have shown that the side chain of a lysine residue, located in the β-strand $\beta 7$ and strictly conserved in α subunits of nicotinic receptors, systematically moves upon agonist binding, suggesting that it might be involved in both binding and gating. To test this hypothesis in neuronal nicotinic receptors, Lys145 was substituted by other amino acids in the $\alpha 7$ nicotinic receptor, and expression levels and electrophysiological responses for several nicotinic agonists and antagonists were determined. Substitutions of Lys145 showed a variety of functional effects: 1) strong reductions in the functional responses to acetylcholine, nicotine, and dimethylphenylpiperazinium, the latter becoming an antagonist; 2) increases in the agonist EC_{50} values (up to 80-fold with acetylcholine); 3) heterogeneous behavior of the different agonists, with epibatidine and cytisine being less affected by the substitutions; 4) decreases of agonist affinities for the desensitized receptors; and 5) small changes in the affinity of nicotinic antagonists. It is concluded that the presence of a polar or positively charged side chain at this position improves the gating function with acetylcholine and nicotine, although the lysine side chain seems to be necessary for retaining the binding properties of acetylcholine. The results are compatible with the involvement of Lys145 in the early steps of channel activation by acetylcholine.

Nicotinic acetylcholine receptors (nAChRs) mediate fast synaptic transmission in nerve and muscle cells, and they are members of the Cys-loop family of ligand-gated ion channels, which includes 5-hydroxytryptamine$_3$, γ-$GABA_A$ receptors, and glycine receptors (Lester et al., 2004). Such receptors are allosteric proteins because the signal generated at the binding site region must be transmitted to the channel gate located some distance away, and this process involves a more than local conformational change. Site-directed mutagenesis has been useful in identifying several residues and domains involved in the mechanisms of coupling agonist binding to channel gating, but the precise molecular mechanisms underlying channel activation remain mainly unclear. Unwin and coworkers have proposed a model of activation in which the interaction of the agonist with the binding site generates a 15° clockwise rotation of the α subunits that is transmitted to the gate through rearrangements of several extracellular structures, mainly loops 2 and 7 (Cys-loop) and the M2-M3 linker (Miyazawa et al., 2003; Unwin, 2005). This hypothesis is supported by functional data obtained in several Cys-loop receptors, such as $GABA_A$ receptors (Sigel et al., 1999; Bera et al., 2002; Kash et al., 2003), glycine receptors (Rajendra et al., 1995; Lynch et al., 1997; Absalom et al., 2003; Schofield et al., 2003), and nAChRs (Grosman et al., 2000a; Chakrapani et al., 2004), including the neuronal subtype (Campos-Caro et al., 1996; Sala et al., 2005). Of particular interest is the analysis of linear free energy relationships based on muscle nAChR single-channel data, which suggest that during gating dozens of residues are organized into rigid body gating domains that move asynchronously, proceeding like a "conformational wave" (Grosman et al., 2000b; Auerbach, 2005).

The crystal structure of a snail acetylcholine binding protein (AChBP) has been resolved and offers new insights into

This work was supported by grants from the Ministry of Science and Technology of Spain (BMC2002-00972 and SAF2002-00209) and the Generalitat Valenciana (CTIDIB/2002/138 and GRUPOS03/038).

Article, publication date, and citation information can be found at http://molpharm.aspetjournals.org.

doi:10.1124/mol.105.015446.

ABBREVIATIONS: nAChR, nicotinic acetylcholine receptor; AChBP, acetylcholine binding protein; α-Bgt, α-bungarotoxin; ACh, acetylcholine; MLA, methyllycaconitine; DHβE, dihydro-β-erythroidine; dTC, *d*-tubocurarine; DMPP, dimethylphenylpiperazinium.

the molecular mechanisms involved in binding and coupling of nAChRs (Brejc et al., 2001). For example, a conserved lysine residue at the β-strand β7 (equivalent to Lys145 in the bovine α7 subunit) has been located close to both the Cys-loop and the binding segment C, the latter containing several aromatic residues involved in binding of nicotinic agonists and antagonists (Galzi et al., 1991; Brejc et al., 2001). Moreover, the crystallographic data have also shown that, upon binding of nicotinic agonists to AChBP, the side chain of such a lysine residue moves systematically to form a hydrogen bond to the hydroxyl group of the conserved Tyr185 at the binding segment C (Celie et al., 2004). Because of its crucial position, it is suggested that Lys145 could play an important role in both binding and gating of nAChRs. We have checked this hypothesis by constructing α7 receptors mutated at position 145 and analyzing their whole-cell responses to several nicotinic ligands. This report shows that mutations of amino acid Lys145 result in large and ligand-dependent changes in both efficacy and potency of several nicotinic agonists and antagonists, supporting a key role of this residue in both binding and its transduction into channel activation of nAChR in a ligand-dependent manner.

Materials and Methods

Generation of Mutants of the Bovine α7 Subunit. The bovine α7 cDNA (Garcia-Guzman et al., 1995) was cloned in a derivative of the pSP64T vector (Krieg and Melton, 1984) containing part of the pBlueScript polylinker (Stratagene, La Jolla, CA). The appropriate DNA cassettes were generated by polymerase chain reaction (25 cycles at 94°C for 10 s, 60°C for 30 s, and 72°C for 45 s) and used to substitute original segments of the α7 subunit, by performing restriction enzyme digestions. For this purpose, silent mutations were introduced to generate two restriction enzyme sites useful for mutant construction: an AatII site corresponding to amino acids Asp138 and Val139 and a BamHI site involving amino acids Gly147 and Ser148. To generate the mutants, we annealed single-stranded oligonucleotides with the desired sequences and proper single strand ends, which could be easily ligated to the ends generated by the restriction enzymes mentioned above.

Oocyte Expression. Capped mRNA was synthesized in vitro using SP6 RNA polymerase, the mMESSAGEmMACHINE kit (Ambion, Austin, TX), and the pSP64T derivative mentioned above. Defoliculated *Xenopus laevis* oocytes were injected with 5 ng of total cRNA in 50 nl of sterile water. All experiments were performed within 3 to 4 days after cRNA injection. Wild-type α7 mRNA was injected into oocytes from the same frog every time a mutant was tested. Consequently, mutant expression was expressed as a percentage of wild-type α7 expression observed in the same experiment.

^{125}I-α-Bungarotoxin Binding Assays. Specific surface expression of ^{125}I-α-bungarotoxin (α-Bgt) (GE Healthcare, Little Chalfont, Buckinghamshire, UK) binding sites was tested with 5 nM ^{125}I-α-Bgt as described previously (Garcia-Guzman et al., 1994). In brief, oocytes were incubated with 5 nM ^{125}I-α-Bgt for 2 h at 18°C. At the end of the incubation, unbound ^{125}I-α-Bgt was removed, oocytes were washed, and bound radioactivity was counted. Nonspecific binding was determined using noninoculated oocytes. For displacement experiments, oocytes were preincubated with increasing concentrations of agonists during 15 min followed by incubation with 1 nM ^{125}I-α-Bgt, always in the presence of agonists. After 2 h, oocytes were treated as described above.

Electrophysiological Recordings. Electrophysiological recordings were done as described previously (Garcia-Guzman et al., 1994; Campos-Caro et al., 1997; Sala et al., 2002). In brief, oocytes were located in a chamber (0.9-ml volume) and perfused by gravity with a modified frog Ringer's solution containing 82.5 mM NaCl, 2.5 mM KCl, 2.5 mM $BaCl_2$, 1 mM $MgCl_2$, and 5 mM HEPES, pH 7.4. Perfusion rate was 12 to 15 ml/min. Agonists were applied through a gravity-driven pipette with an internal diameter of 1.2 mm and located close to the animal hemisphere of the oocyte. The velocity of application was 18 to 22 ml/min. The solution exchange rate followed an exponential time course with $\tau_f = 90 \pm 5$ ms. Holding potential was usually −80 mV. Most experiments were done using 30 μM epibatidine as the control response. Currents were filtered at 50 Hz with a low-pass eight-pole Bessel filter, sampled at 100 to 500 Hz, and stored on hard disk for later analysis. Data acquisition and agonist application were controlled by a DigiData 1200 interface driven by pClamp 6.0 software (Molecular Devices, Sunnyvale, CA). All experiments were done at room temperature (22°C).

Data Analysis. Current amplitudes were measured at the peak inward current, and no correction for desensitization or solution exchange rate was made because our control results were very close to those reported after correction (Papke and Porter Papke, 2002). Although they would not be true values, it was assumed that estimates of maximal responses and potency of agonists can be compared on a pairwise basis by null methods (Colquhoun, 1998). Unless otherwise indicated, current amplitudes upon stimulation with different concentrations of the agonists studied were first normalized to their internal control obtained with 30 μM epibatidine, which yielded near maximal responses in all receptors. Although the magnitude of the control currents was usually stable, sometimes they run down slowly along the experiment; thus, percentages of the control currents were calculated over the interpolated control current. Data analysis was performed with the software package Prism 4.0 (GraphPad Software Inc., San Diego, CA). EC_{50} and maximal current (I_{max}) values were calculated by nonlinear regression analysis using the Hill equation: $I/I_{max} = 1/[1 + (EC_{50}/C)^{n_H}]$, where EC_{50} is the agonist concentration that elicits the half-maximal response, n_H is the Hill coefficient, and C is the agonist concentration. Inhibition by antagonists and displacement curves were fitted by the Hill equation with $n_H = -1$, obtaining IC_{50} values that were converted to K_i values using a variant of the Cheng-Prusoff equation (Leff and Dougall, 1993). For the sake of overall comparison, estimates of the gating function were normalized to the maximal response to epibatidine in wild-type receptors as shown in concentration-response curves and Table 2. More precisely, functional expression of the different receptor-agonist pairs was obtained from the I_{max} values extracted from the Hill equation (always referred to the response with 30 μM epibatidine). Then, these values were corrected to account for differences in both the potency of epibatidine and the level of surface expression in the different receptors. Results are presented as means and S.E.

Chemicals. Unless otherwise indicated, all chemicals were purchased from Sigma-Aldrich (St. Louis, MO).

Results

Effect of the Mutation K145A on Functional Responses Evoked by Acetylcholine. Residue Lys145, which is close to the Cys-loop of α7 nAChR, was mutated to alanine, a substitution that should cause minimal disruption to the receptor secondary structure. Functional responses were initially tested by recording ionic currents evoked by acetylcholine (ACh), and they were very different from the control. Figure 1A shows a family of ACh-evoked ionic currents in control and K145A receptors. Several changes could be observed in mutant K145A: 1) higher ACh concentrations were needed to evoke functional responses, 2) ionic currents in mutant K145A were much smaller than in control, and 3) decay kinetics were slower even when equipotent ACh concentrations were used. For example, half-decay times were 117 ± 12 ms ($n = 13$) and 250 ± 74 ms ($n = 3$) in control (1

mM ACh) and mutant K145A (30 mM ACh), respectively. However, because mutations might affect not only functional responses but also nAChR assembly and/or transport, surface expression of nAChRs was also monitored by measuring α-Bgt binding sites at the external surface of oocytes. Control oocytes expressed 10.9 ± 1.7 fmol of α-Bgt, and the expression of mutant K145A was around 74% of control (Table 1). Hereafter, all functional responses of mutants have been corrected for surface expression, as in Table 2 and Fig. 6. The functional response of mutant K145A to ACh decreased to 21% of control. The EC_{50} of ACh increased from 38 μM (control) to 1600 μM (mutant K145A). Although from macroscopic concentration-response curves alone it is not possible to deduce for certain how the receptor is affected by the mutation (see *Discussion*), the decrease in maximal currents and the considerable increase in EC_{50} suggest that mutation of Lys145 has changed both the binding and the gating properties of the mutant nAChRs when ACh was the agonist.

Effect of the Mutation K145A on Functional Responses Evoked by Other Nicotinic Agonists. To explore whether the effects observed with ACh were shared by other nicotinic agonists, concentration-response curves were obtained with epibatidine, dimethylphenylpiperazinium (DMPP), nicotine, and cytisine as agonists. In wild-type receptors, all four agonists gave functional responses of magnitude very similar to that of ACh (range 94–111% with respect to the maximal response evoked by epibatidine; Table 2) and with similar decay kinetics (not shown), although with a wide range of differences in potency, epibatidine being the most potent agonist (EC_{50} = 1.9 μM) and nicotine the less potent agonist (EC_{50} = 101 μM). Figure 2 shows several patterns of change in the pharmacological properties of agonists when activating mutant K145A. Concerning the maximal evoked response, nicotine behaved much like ACh, reducing its effectiveness to 16%. In contrast, epibatidine response was only reduced to 65%, whereas cytisine conserved most of its effectiveness (91%). Decay kinetics in mutant K145A remained consistently unchanged when the agonists used were either epibatidine or cytisine (data not shown). In contrast, as occurred with ACh, decay kinetics were slowed down in nicotine-evoked responses; half-decay time increased from 68 ± 9 ms (control, 300 μM; n = 4) to 165 ± 4 ms (K145A, 3000 μM; n = 3). The extent of the changes in potency was also dependent on the agonist used. Epibatidine and nicotine increased their EC_{50} around 4-fold, whereas the change in the cytisine potency was almost of 1 order of magnitude.

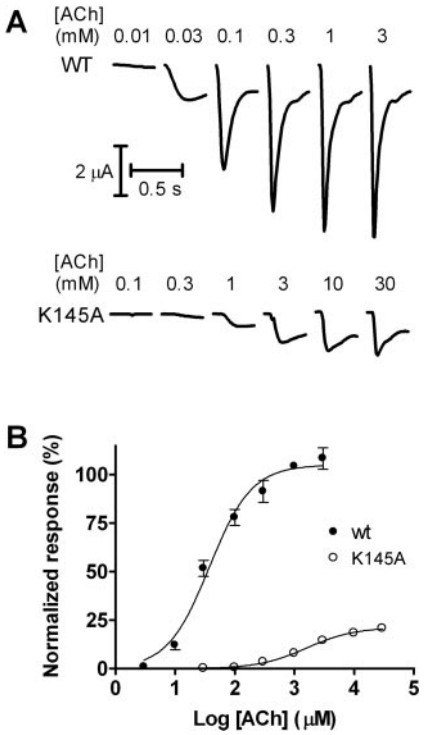

Fig. 1. Comparison between the ACh responses of wild-type α7 nAChR and mutant K145A. A, inward currents obtained upon 1-s stimulation with ACh of wild-type α7 (wt) nAChR and K145A mutants. Traces represent currents obtained at −80 mV with the ACh concentrations indicated on top. B, ACh concentration-response curves of oocytes expressing wild-type α7 (wt, ●) nAChR and K145A mutants (○) for ACh. Data are normalized to the estimated maximal response to epibatidine in wild-type receptors as explained under *Materials and Methods*. Data points represent means ± S.E.M. obtained in four to seven oocytes from three donors. Error bars shown if bigger than symbols. Continuous lines represent fits of data to the Hill equation (see Table 2 for relative I_{max}, EC_{50}, and Hill coefficient values).

A special case occurred when using DMPP as agonist. Mutant K145A did not respond with detectable ionic currents upon stimulation with a wide range of DMPP concentrations. To resolve whether DMPP has lost its affinity for these receptors, or only its ability to activate them, an inhibition curve was constructed. Figure 3 shows that when coapplying DMPP with 3 μM epibatidine, ionic currents were inhibited in a DMPP concentration-dependent manner. The curve could be fitted by a Hill equation with IC_{50} = 19 μM, yielding an apparent K_i of 23 μM. These results show the change in the pharmacological profile of DMPP from full agonist to competitive antagonist in mutant K145A, and reinforce the idea that coupling mechanisms are deeply altered for some, but not all, agonists in mutant K145A.

Effect of the Mutation K145A on the Potency of Nicotinic Antagonists. To examine whether *competitive* nicotinic antagonists have changed their properties in mutant K145A, inhibition curves of the α7-selective antagonist methyllycaconitine (MLA), dihydro-β-erythroidine (DHβE), and *d*-tubocurarine (dTC) were obtained in wild-type and mutant K145A nAChRs. When these antagonists were coapplied with 3 μM epibatidine, responses were inhibited in a concentration-dependent manner in both receptors (Fig. 4). However, the potencies of all antagonists were higher in mutant K145A, especially with dTC. Values of IC_{50} for MLA were 1.2 nM and 55 pM in control and mutant K145A, respectively. This represented a 6-fold decrease in the K_i value for MLA in the mutant K145A (from 0.43 nM to 71 pM). The increase in antagonist potency was larger with dTC, showing a 15-fold decrease in the K_i value in the mutant K145A (from 2.9 to 0.19 μM). Moderate figures were obtained with DHβE, in that its calculated K_i value decreased only from 10 to 6.0 μM. In contrast with these results, the nonselective, noncompetitive channel blocker mecamylamine did not show any change in its potency (K_i values of 5.8 and 7.2 μM in control and mutant K145A receptors, respectively; data not shown).

Changes in Desensitization Paralleled Those of Activation in Mutant K145A. The decreases in maximal currents observed with ACh and nicotine could be caused by impaired gating as pointed out above, but they could also be due to an enhancement of agonist-induced desensitization,

especially in systems where the solution exchange time course is similar to that of desensitization. Thus, desensitization over a range of agonist concentrations was examined. Figure 5A shows the responses of wild-type and mutant K145A receptors to 3 μM epibatidine when previously exposed to 3-min incubation periods with different ACh concentrations. Control responses were inhibited by the pre-exposure of increasing ACh concentrations with an IC_{50} = 4.0 μM (Fig. 5B). In mutant K145A, the ACh desensitization curve was shifted to the right by more than 1 order of magnitude (IC_{50} = 185 μM). This is in quantitative agreement with the shift observed in the concentration-response curve of ACh and suggests that the affinities of active and desensitized conformations in mutant K145A for ACh have changed similarly. Moreover, these data rule out the possibility that decreases in peak currents might have been caused by agonist-induced fast desensitization, which would have appeared in mutant K145A as a new feature. When nicotine was used as the desensitizing agonist, a right shift of the curves was also observed (Fig. 5C). An increase in IC_{50} value from 4.0 to 15 μM was again in fair agreement with the shift observed in the activation curve. Quantitatively similar results were obtained with epibatidine and cytisine in mutant K145A (not shown)

A complementary approach to study the affinity of agonists for the desensitized conformations of the receptors is by means of obtaining α-Bgt displacement experiments. In such conditions, a mixture of resting, active, and desensitized states is supposed to be at equilibrium, although a higher proportion of the desensitized states is expected because of the continuous exposure to the agonists. Figure 6 shows the displacement curves of 1 nM α-Bgt by acetylcholine and epibatidine in both control and mutant receptors. Higher concentrations of both agonists were needed to compete with the toxin in the mutant K145A, so a shift to the right was observed in both displacement curves. Data were fitted by the Hill equation with negative slope, and the values of IC_{50} were used to calculate the corresponding K_i values. It should be pointed out that α-Bgt affinity was slightly higher in mutant K145A, because the K_D value changed from 1.4 to 0.56 nM (data not shown). Calculation of the acetylcholine K_i yielded values of 6.5 and 149 μM in control and mutant K145A, respectively. Such a 23-fold decrease in the apparent affinity of acetylcholine for these prevalently desensitized conformations is in agreement with previous results. For epibatidine, the effect of the mutation was smaller, because only a 9-fold change in the calculated K_i was obtained (0.15 and 1.4 μM in control and mutant K145A, respectively).

Other Substitutions at Position 145 Show Diverse Effects on Binding and Gating. To examine more closely the effects of the residues at position 145, three other mutants were constructed and analyzed as described above. These were mutants K145Q; K145R, which conserved the positive charge of lysine; and K145E, which reversed the positive charge. All mutants were well expressed in oocytes (Table 1), but each gave rise to different degrees of functional expression. Figure 7 shows a family of ACh-evoked ionic currents in each of these three mutant receptors. Note that, to estimate the gating function, the magnitude of the currents should be corrected for the level of surface expression of each mutant. Thus, it could be observed that mutant K145E showed smaller currents that were associated with slower

TABLE 1

Surface and functional expression of wild-type and Lys145 mutant nAChRs

Surface expression is given as percentages of the number of α-Bgt binding sites in wild-type receptors. Functional expression was measured upon stimulation with 30 μM epibatidine of 22 to 31 oocytes (five donors) expressing the different nAChRs. Values shown are mean ± S.E.

	α7 wt	α7 K145A	α7 K145R	α7 K145Q	α7 K145E
Surface expression (%)	100 ± 16	74 ± 1	114 ± 15	186 ± 2	318 ± 1
Functional expression (μA/oocyte)	7.3 ± 0.1	3.4 ± 0.1	4.4 ± 0.1	8.5 ± 0.2	10.6 ± 0.1

wt, wild-type.

TABLE 2

Pharmacological properties of wild-type and Lys145 mutant nAChRs

Values shown are parameters ± S.E. obtained by fitting data to the Hill equation. Data were obtained from four to 10 oocytes (at least two donors). I_{max} values are corrected for surface expression and normalized to the estimated maximal response with epibatidine in wild-type nAChRs.

	α7 wt	α7 K145A	α7 K145R	α7 K145Q	α7 K145E
Epibatidine					
I_{max} (%)	100 ± 1	65 ± 1	58 ± 1	52 ± 1	40 ± 1
EC_{50} (μM)	1.9 ± 0.4	6.6 ± 0.7	9.9 ± 1.2	2.8 ± 1.5	6.9 ± 0.7
n_H	0.9	1.4	1.4	0.9	1.8
ACh					
I_{max} (%)	102 ± 2	21 ± 1	67 ± 4	67 ± 10	8.0 ± 0.5
EC_{50} (μM)	38 ± 5	1600 ± 170	3100 ± 610	600 ± 260	1040 ± 140
n_H	1.3	1.1	1.0	1.1	1.6
Nicotine					
I_{max} (%)	110 ± 10	16 ± 3	33 ± 2	39 ± 2	3.0 ± 0.2
EC_{50} (μM)	101 ± 34	470 ± 270	290 ± 40	300 ± 50	240 ± 40
n_H	1.1	1.0	1.6	1.4	1.6
Cytisine					
I_{max} (%)	94 ± 4	88 ± 3	58 ± 8	52 ± 2	46 ± 2
EC_{50} (μM)	28 ± 4	240 ± 20	93 ± 52	46 ± 7	190 ± 30
n_H	1.9	1.5	0.9	1.4	1.4
DMPP					
I_{max} (%)	101 ± 6	0	31 ± 6	7 ± 1	0.3 ± 0.1
EC_{50} (μM)	12 ± 2	N.D.	220 ± 140	5.2 ± 1.7	5.8 ± 2.9
n_H	1.1	N.D.	0.8	1.2	1.4

N.D., not determined; wt, wild-type.

desensitization kinetics, as occurred with mutant K145A. Data in Table 2 show the varied effects of these substitutions on binding and gating once the respective level of surface expression has been considered. Compared with control, the mutant K145R showed reductions in the maximal currents for all five agonists tested. However, when the agonists were epibatidine, cytisine, or ACh, the magnitude of these currents was comparable with those obtained in control receptors (58–67%). With nicotine and DMPP, the functional response decayed to around 32% of control. Nevertheless, the more striking feature of mutant K145R was the right shift of ACh concentration-response curve (and to a lesser extent the curve for DMPP) by almost 2 orders of magnitude, changing the EC_{50} value from 38 μM to 3.1 mM for ACh (from 12 to 223 μM for DMPP). These results are in contrast with those obtained with the other agonists with only 3- to 5-fold increases in the EC_{50} values. Affinities of nicotinic antagonists DHβE and dTC were also explored in mutant K145R. As in mutant K145A, the affinity of both antagonists increased slightly as calculated K_i values decreased 3-fold for DHβE and 4-fold for dTC (data not shown).

Results obtained in mutant K145Q show that the maximal responses decreased similarly for all agonists (40–50% of control) except DMPP, which showed a relative efficacy of only 7%. Moreover, the concentration-response curves in this mutant are less changed with respect to the control. Finally, in mutant K145E, maximal responses decreased for ACh (7%), nicotine (3%), and DMPP (<1%), resembling the results obtained in mutant K145A. The most changed EC_{50} value was again that of ACh (27-fold increase). Like in other mutants, the secondary amines epibatidine and cytisine were the agonists less affected in both their EC_{50} values and magnitude of responses. It should be noted that Hill coefficients showed large variations among the different mutants and different agonists, which are not expected to be derived from changes in gating alone. This lack of correlation would be explained if mutations also affected binding cooperativity, although there is no unequivocal evidence of this effect. Concerning the decay kinetics, the same pattern shown by mutant K145A was observed; i.e., when equipotent agonist concentrations were compared, decay kinetics was similar for agonists whose functional responses were less affected (epibatidine and cytisine but also ACh in mutants K145R and K145Q) but slowed down when functional responses were strongly reduced as in mutant K145E.

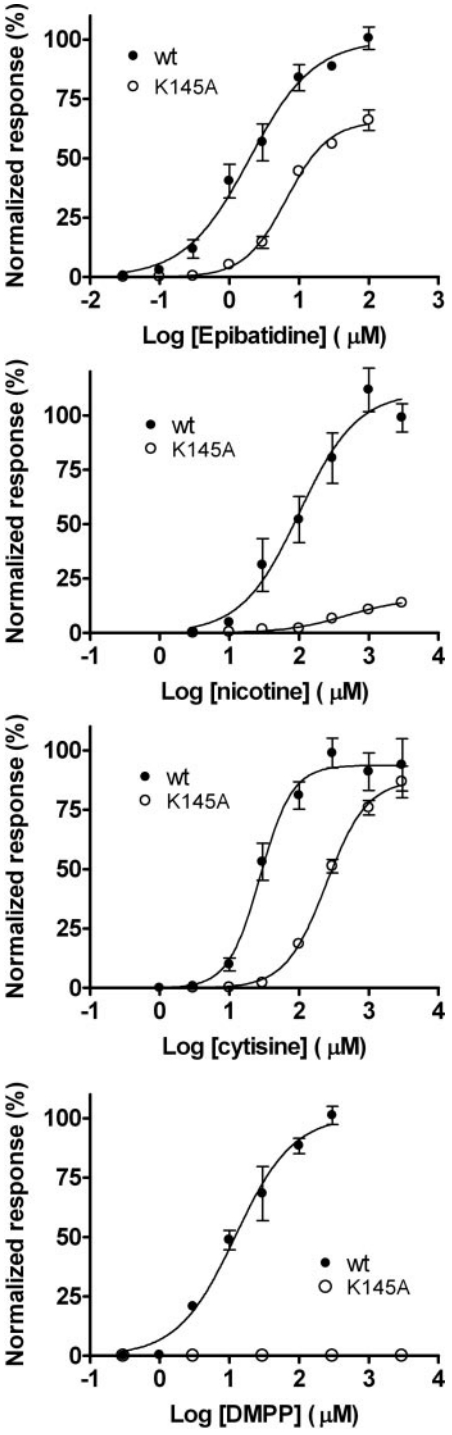

Fig. 2. Pharmacological profile of several nicotinic agonists in wild-type α7 nAChR and mutant K145A. Concentration-response curves of oocytes expressing wild-type α7 (wt, ●) nAChRs and mutant K145A (○) for epibatidine, nicotine, cytisine, and DMPP. Data are normalized to the estimated maximal response to epibatidine in wild-type receptors as explained under *Materials and Methods*. Data points represent means ± S.E.M. obtained in four to eight oocytes from two to three donors. Error bars are shown if they are bigger than symbols. Continuous lines represent fits of data to the Hill equation (see Table 2 for relative I_{max}, EC_{50}, and Hill coefficient values).

Discussion

The fine molecular mechanisms involved in channel activation of Cys-loop receptors are not well established. However, a model of activation has been proposed in which the

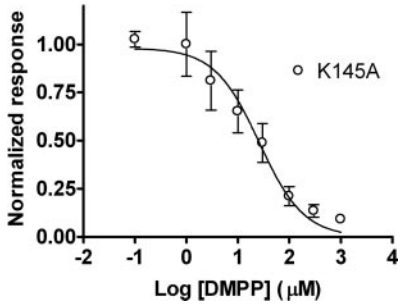

Fig. 3. DMPP is an antagonist in mutant K145A. Concentration dependence in the DMPP inhibition of ionic currents evoked by 3 μM epibatidine in oocytes expressing mutant K145A. Data are means ± S.E.M. of six oocytes (two donors). Continuous line represents a fit to the Hill equation ($n_H = -1$) with an IC_{50} value of 19 μM.

interaction of the agonist with the binding site is transmitted to the gate through rearrangements of several extracellular structures, including the Cys-loop (Miyazawa et al., 2003; Unwin, 2005). Structural data from the snail AChBP indicated that the residue equivalent to α7 Lys145 moves toward the hydroxyl group of Tyr185 upon agonist binding (Celie et al., 2004). In nAChR α subunits, the equivalent tyrosine residue, Tyr190 in α7 nAChRs, has been shown to be critical for ACh binding, channel gating, and desensitization (Galzi et al., 1991; Sine et al., 1994; Chen et al., 1995). Besides, the mentioned lysine is conserved in α subunits and is located close to the Cys-loop. Because of its strategic location, we have tested the hypothesis that Lys145 in α7 nAChRs might play an important role in binding of nicotinic agonists and/or in the coupling mechanisms involved in channel opening by analyzing functional responses of several mutants.

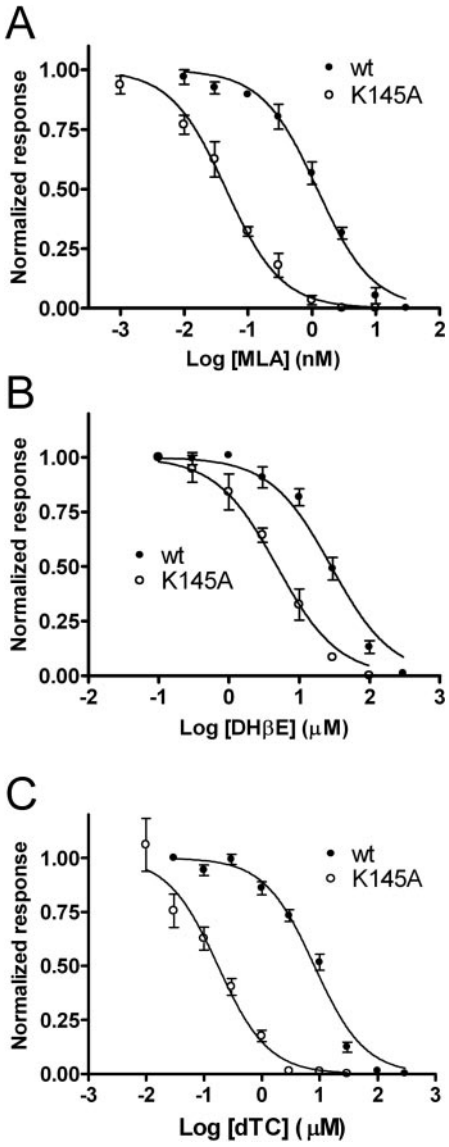

Fig. 4. Inhibition curves of nicotinic antagonists in wild-type α7 nAChR and mutant K145A. A, MLA inhibition of ionic currents evoked by 3 μM epibatidine in oocytes expressing wild-type α7 (wt, ●) nAChR and mutant K145A (○). Data are means ± S.E.M. of three to four oocytes (two donors). Continuous lines represent fits to the Hill equation ($n_H = -1$) with IC_{50} values of 1.2 and 0.045 nM (K_i values of 430 and 71 pM) for wild-type and mutant K145A, respectively. B, DHβE inhibition of ionic currents evoked by 3 μM epibatidine in oocytes expressing wild-type α7 (wt, ●) nAChR and mutant K145A (○). Data are means ± S.E.M. of five to six oocytes (two donors). Continuous lines represent fits to the Hill equation ($n_H = -1$) with IC_{50} values of 28 and 4.8 μM (K_i values of 10 and 6.0 μM) for wild-type and mutant K145A, respectively. C, *d*-tubocurarine inhibition of ionic currents evoked by 3 μM epibatidine in oocytes expressing wild-type α7 (wt, ●) nAChR and mutant K145A (○). Data are means ± S.E.M. of six to nine oocytes (three donors). Continuous lines represent fits to the Hill equation ($n_H = -1$) with IC_{50} values of 8.1 and 0.15 μM (K_i values of 2.9 and 0.19 μM) for wild-type and mutant K145A, respectively. Error bars are shown if they are bigger than symbols.

Conclusions drawn from concentration-response curves are limited by several factors, including the number of functional receptors, the presence of desensitization and/or channel block, and the binding-gating problem (Colquhoun, 1998). However, these concerns have been addressed in this study. First, the magnitudes of the functional responses were normalized by the levels of surface expression. Second, currents evoked upon continuous application of high agonist concentrations decayed with the same time course, regardless of both the receptor and the agonist studied, except in some cases in which the reduction in maximal responses was accompanied by a slightly slower time course of macroscopic desensitization. This would indicate that the true reductions in both maximal response and potency might be larger than observed, reinforcing our conclusions. Third, current-voltage relationships with 3 mM ACh in wild-type and mutant K145A were indistinguishable (data not shown), suggesting that open-channel block is not increased in mutants. Finally, reductions in maximal response could arise from fast entry into a desensitized state that would remain undetected, were it facilitated in mutants, because of the slow exchange solution rate. According to this possibility, continuous exposure to low agonist concentrations should produce more desensitization in mutants than in wild-type receptors, but the concentration-desensitization curves showed just the opposite effect. Therefore, we have considered maximal response as an efficient indicator of gating mechanisms when comparing different receptor-agonist pairs.

The large reductions in the functional responses measured in mutant nAChRs suggest that the conformational changes involved in gating are impaired by the amino acid substitutions. In mutant K145A, the secondary amines cytisine and epibatidine retained most of their effectiveness, but functional responses with nicotine and ACh were strongly decreased. With DMPP, the reduction in gating function was total because this nicotinic ligand lost its ability to activate mutant K145A but not to inhibit epibatidine responses. When the amino acid substitution was more conservative, as in mutant K145R, functional responses to the most affected agonists in mutant K145A (ACh, nicotine, and DMPP) were partially restored, suggesting that their coupling mechanisms (but not the mechanisms for cytisine and epibatidine) are favored when a positive charge is present at position 145. This is further supported by the opposite results obtained with the reverse mutant K145E. In this case, the presence of a negative charge strongly impaired the gating function of ACh, nicotine, and DMPP, but it affected only moderately that of cytisine and epibatidine. Finally, an intermediate situation was found in mutant K145Q. The presence of the glutamine residue might have created a sufficiently polar environment that results in responses similar to the responses shown by mutant K145R for all agonists (except for DMPP).

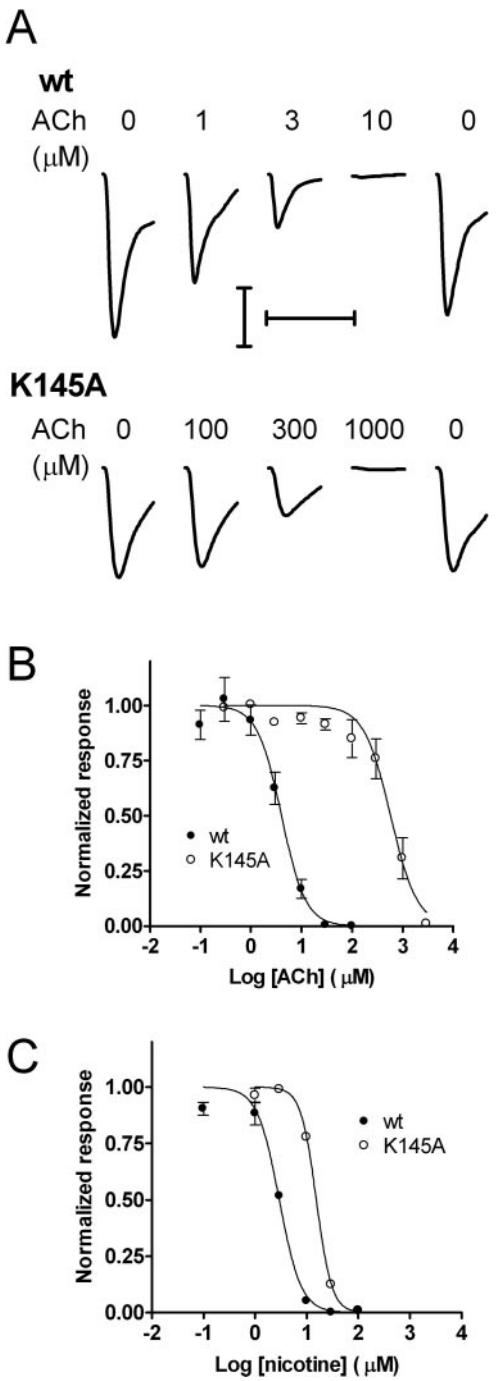

Fig. 5. Mutant K145A is less sensitive to desensitization by low concentrations of agonists. A, ionic currents evoked by 3 μM epibatidine in two representative oocytes expressing wild-type α7 nAChR and mutant K145A. Oocytes were exposed during 3 min to the indicated ACh concentration before epibatidine stimulation. Time between pulses was 6 min, which allows full recovery from desensitization. Scale bars, 1 s and 1 or 3 μA for wild-type and mutant K145A, respectively. B, concentration-response curves of the epibatidine-evoked fractional current remaining after 3-min ACh exposure in oocytes expressing wild-type α7 (●) nAChR and mutant K145A (○). Data are means ± S.E.M. of three to six oocytes (two to three donors). Continuous lines represent fits to the Hill equation with IC_{50} values of 4.0 μM ($n_H = -1.76$) and 185 μM ($n_H = -1.82$) for wild-type and mutant K145A, respectively. C, concentration-response curves of the epibatidine-evoked fractional current remaining after 3-min nicotine exposure in oocytes expressing wild-type α7 (●) nAChR and mutant K145A (○). Data are means ± S.E.M. of three to four oocytes (two donors). Continuous lines represent fits to the Hill equation with IC_{50} values of 3.0 μM ($n_H = -2.0$) and 15 μM ($n_H = -2.9$) for wild-type and mutant K145A, respectively.

If a simple kinetic scheme is used to explain the concentration-response data (Colquhoun, 1998), the changes observed in the EC_{50} values of these agonists in mutant K145A are somewhat larger than predicted by a selective effect on gating mechanisms. Considering that most of the deviations are not large and also the limitations of our experimental setup, it is difficult to draw conclusions about potential changes in agonist binding properties. As an exception, the increase in the EC_{50} of ACh in mutant K145A was 42-fold. Such an effect largely exceeds what would be expected from a gating modification alone, suggesting that binding properties of ACh have been changed as well. This was further confirmed in mutant K145R, because the gating function of ACh was rather unaffected, but the increase in EC_{50} was the largest (>80-fold). These results suggested that the interaction of ACh (but not of other ligands) with the binding site is extremely dependent on Lys145. According to data from AChBP, the interaction between Lys145 and Tyr190 would affect the ligand affinity through a readjustment of the Tyr190 side chain (Celie et al., 2004). This seems to be true for ACh because large shifts on the concentration-response and desensitization curves were observed upon substitution of Lys145. In contrast, we have not detected large shifts on the nicotine curves. The discrepancy could be partly ex-

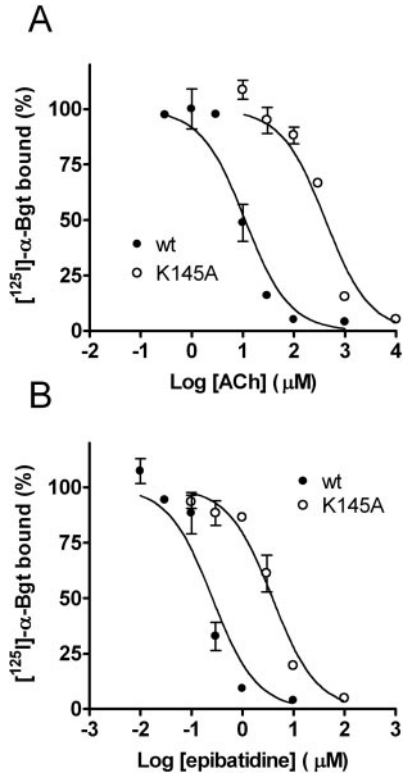

Fig. 6. Binding properties of the desensitized conformation of wild-type α7 nAChR and mutant K145A. A, ACh displacement curves of bound α-Bgt from oocyte plasma membranes expressing wild-type α7 (●) nAChR and mutant K145A (○). Data are means ± S.E.M. of three experiments (three donors) with 10 to 15 oocytes each. Continuous lines represent fits to the Hill equation ($n_H = -1$) with IC_{50} values of 11 and 414 μM (K_i values of 6.5 and 149 μM) for wild-type and mutant K145A, respectively. B, epibatidine displacement curves of bound α-Bgt from oocyte plasma membranes expressing wild-type α7 (●) nAChRs and mutant K145A (○). Data are means ± S.E.M. of three experiments (three donors) with 10 to 15 oocytes each. Continuous lines represent fits to the Hill equation ($n_H = -1$) with IC_{50} values of 0.25 and 3.9 μM (K_i values of 0.15 and 1.4 μM) for wild-type and mutant K145A, respectively.

plained if, as occurred in AChBP, the Tyr190 side chain would interact with the carbons of the choline group of ACh but not with those of nicotine (Celie et al., 2004). All checked competitive antagonists showed consistent increases in their affinity, suggesting again that Lys145 influences the interaction of ligands with the binding site.

Thus, Lys145 could play a role in both binding and gating of homomeric nAChRs, as reported for some other residues located at the extracellular domain of a variety of Cys-loop receptors (Galzi et al., 1991; Chen et al., 1995; Sine et al., 2002; Grutter et al., 2003; Beene et al., 2004; Newell et al., 2004). An interaction between Lys145 and the binding segments may be an initial trigger for ion channel activation, transducing a change into the neighboring Cys-loop that is an important part of the channel opening mechanism (Chakrapani et al., 2004; Sala et al., 2005). In good agreement with the results shown here, it has been recently reported the effects of mutations of a lysine residue equivalent to Lys145 on gating of muscle-type nicotinic receptors upon ACh activation (Mukhtasimova et al., 2005). This report shows drastic effects on gating after substitutions on position 145 and proposes that the interaction between the conserved residues Lys142, Tyr190, and Asp200 would initiate the conformational changes leading to channel activation. These authors also report effects on ACh binding, although smaller than those presented here. This quantitative difference could be due to the different receptors studied and/or to some assumptions about binding steps made in the analysis of single-channel data (Mukhtasimova et al., 2005).

It is noteworthy that the analysis of different mutants and several agonists presented here has also revealed significant differences among the agonists used, indicating that the involvement of Lys145 in binding and/or gating is strongly dependent on the nature of the activating molecule. In particular, the efficiency of the natural neurotransmitter ACh is strongly affected even by a conservative substitution of Lys145 and helps to explain why this residue has been conserved in nAChRs. On the other hand, coupling of binding to gating with the secondary amines epibatidine or cytisine seems to be rather independent of the nature of the side chain at position 142.

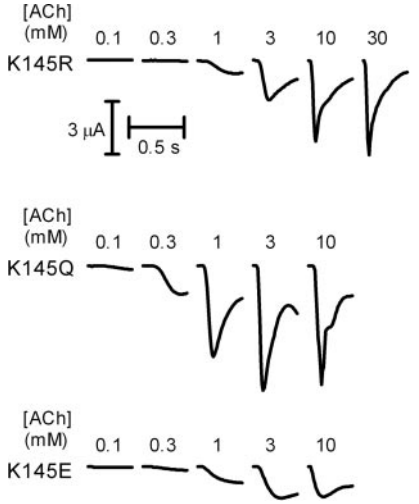

Fig. 7. Functional responses of K145 mutants to ACh. From top to bottom, inward currents obtained upon 1-s stimulation with ACh of three representative oocytes expressing K145R, K145Q, and K145E mutants, respectively. Traces represent currents obtained at −80 mV with the ACh concentrations indicated on top. Scale bars apply to all traces. Note that for proper comparison, current magnitudes should be corrected by the level of surface expression.

Coupling mechanisms in neuronal nAChRs may be specific of agonist, at least in the early rearrangements. According to that, several residues and/or regions of the extracellular domain of α and β subunits have been identified in neuronal nAChRs as determinants of the sensitivity to agonists such as cytisine (Luetje and Patrick, 1991; Figl et al., 1992; Papke and Heinemann, 1994), DMPP (Anand et al., 1998), and nicotine (Hussy et al., 1994). On the other hand, previous work with single point mutations in the loop 2, the Cys-loop, and the M2-M3 linker of α7 nAChRs has shown that coupling mechanisms were equally affected for different nicotinic agonists (Campos-Caro et al., 1996; Sala et al., 2005). The difference between these two sets of results might be due to the precise location of the mutated or swapped residues with respect to the binding domains. In the former group, they might be located close to the binding domain, and in the latter, they are proposed to be parts of the mechanical engagement between extracellular and intramembrane domains (Corringer et al., 2000; Lester et al., 2004; Unwin, 2005). The conserved Lys145 belongs to the first group; therefore, it is likely to be involved in pharmacological selectivity, mostly by conditioning the earliest rearrangements involved in the transmission of the conformational wave that will result in gate opening. At the moment, however, both the high complexity of those indirect interactions and the lack of refined structural data make it difficult to establish a clear correlation between the structural and chemical properties of the side chain at position 145 and the resulting pharmacological phenotype.

References

Absalom NL, Lewis TM, Kaplan W, Pierce KD, and Schofield PR (2003) Role of charged residues in coupling ligand binding and channel activation in the extracellular domain of the glycine receptor. *J Biol Chem* **278:**50151–50157.

Anand R, Nelson ME, Gerzanich V, Wells GB, and Lindstrom J (1998) Determinants of channel gating located in the N-terminal extracellular domain of nicotinic α7 receptor. *J Pharmacol Exp Ther* **287:**469–479.

Auerbach A (2005) Gating of acetylcholine receptor channels: Brownian motion across a broad transition state. *Proc Natl Acad Sci USA* **102:**1408–1412.

Beene DL, Price KL, Lester HA, Dougherty DA, and Lummis SC (2004) Tyrosine residues that control binding and gating in the 5-hydroxytryptamine3 receptor revealed by unnatural amino acid mutagenesis. *J Neurosci* **24:**9097–9104.

Bera AK, Chatav M, and Akabas MH (2002) GABA(A) receptor M2–M3 loop secondary structure and changes in accessibility during channel gating. *J Biol Chem* **277:**43002–43010.

Brejc K, van Dijk WJ, Klaassen RV, Schuurmans M, van Der OJ, Smit AB, and Sixma TK (2001) Crystal structure of an ACh-binding protein reveals the ligand-binding domain of nicotinic receptors. *Nature (Lond)* **411:**269–276.

Campos-Caro A, Rovira JC, Vicente-Agullo F, Ballesta JJ, Sala S, Criado M, and Sala F (1997) Role of the putative transmembrane segment M3 in gating of neuronal nicotinic receptors. *Biochemistry* **36:**2709–2715.

Campos-Caro A, Sala S, Ballesta JJ, Vicente-Agullo F, Criado M, and Sala F (1996) A single residue in the M2–M3 loop is a major determinant of coupling between binding and gating in neuronal nicotinic receptors. *Proc Natl Acad Sci USA* **93:**6118–6123.

Celie PH, Rossum-Fikkert SE, van Dijk WJ, Brejc K, Smit AB, and Sixma TK (2004) Nicotine and carbamylcholine binding to nicotinic acetylcholine receptors as studied in AChBP crystal structures. *Neuron* **41:**907–914.

Chakrapani S, Bailey TD, and Auerbach A (2004) Gating dynamics of the acetylcholine receptor extracellular domain. *J Gen Physiol* **123:**341–356.

Chen J, Zhang Y, Akk G, Sine S, and Auerbach A (1995) Activation kinetics of recombinant mouse nicotinic acetylcholine receptors: mutations of alpha-subunit tyrosine 190 affect both binding and gating. *Biophys J* **69:**849–859.

Colquhoun D (1998) Binding, gating, affinity and efficacy: the interpretation of structure-activity relationships for agonists and of the effects of mutating receptors. *Br J Pharmacol* **125:**924–947.

Corringer PJ, Le Novere N, and Changeux JP (2000) Nicotinic receptors at the amino acid level. *Annu Rev Pharmacol Toxicol* **40:**431–458.

Figl A, Cohen BN, Quick MW, Davidson N, and Lester HA (1992) Regions of beta 4.beta 2 subunit chimeras that contribute to the agonist selectivity of neuronal nicotinic receptors. *FEBS Lett* **308:**245–248.

Galzi JL, Bertrand D, Devillers-Thiery A, Revah F, Bertrand S, and Changeux JP

(1991) Functional significance of aromatic amino acids from three peptide loops of the alpha 7 neuronal nicotinic receptor site investigated by site-directed mutagenesis. *FEBS Lett* **294:**198–202.

Garcia-Guzman M, Sala F, Sala S, Campos-Caro A, and Criado M (1994) Role of two acetylcholine receptor subunit domains in homomer formation and intersubunit recognition, as revealed by alpha 3 and alpha 7 subunit chimeras. *Biochemistry* **33:**15198–15203.

Garcia-Guzman M, Sala F, Sala S, Campos-Caro A, Stuhmer W, Gutierrez LM, and Criado M (1995) alpha-Bungarotoxin-sensitive nicotinic receptors on bovine chromaffin cells: molecular cloning, functional expression and alternative splicing of the alpha 7 subunit. *Eur J Neurosci* **7:**647–655.

Grosman C, Salamone FN, Sine SM, and Auerbach A (2000a) The extracellular linker of muscle acetylcholine receptor channels is a gating control element. *J Gen Physiol* **116:**327–340.

Grosman C, Zhou M, and Auerbach A (2000b) Mapping the conformational wave of acetylcholine receptor channel gating. *Nature (Lond)* **403:**773–776.

Grutter T, Prado de Carvalho, Le Novere N, Corringer PJ, Edelstein S, and Changeux JP (2003) An H-bond between two residues from different loops of the acetylcholine binding site contributes to the activation mechanism of nicotinic receptors. *EMBO (Eur Mol Biol Organ) J* **22:**1990–2003.

Hussy N, Ballivet M, and Bertrand D (1994) Agonist and antagonist effects of nicotine on chick neuronal nicotinic receptors are defined by alpha and beta subunits. *J Neurophysiol* **72:**1317–1326.

Kash TL, Jenkins A, Kelley JC, Trudell JR, and Harrison NL (2003) Coupling of agonist binding to channel gating in the GABA(A) receptor. *Nature (Lond)* **421:** 272–275.

Krieg PA and Melton DA (1984) Functional messenger RNAs are produced by SP6 in vitro transcription of cloned cDNAs. *Nucleic Acids Res* **12:**7057–7070.

Leff P and Dougall IG (1993) Further concerns over Cheng-Prusoff analysis. *Trends Pharmacol Sci* **14:**110–112.

Lester HA, Dibas MI, Dahan DS, Leite JF, and Dougherty DA (2004) Cys-loop receptors: new twists and turns. *Trends Neurosci* **27:**329–336.

Luetje CW and Patrick J (1991) Both alpha- and beta-subunits contribute to the agonist sensitivity of neuronal nicotinic acetylcholine receptors. *J Neurosci* **11:** 837–845.

Lynch JW, Rajendra S, Pierce KD, Handford CA, Barry PH, and Schofield PR (1997) Identification of intracellular and extracellular domains mediating signal transduction in the inhibitory glycine receptor chloride channel. *EMBO (Eur Mol Biol Organ) J* **16:**110–120.

Miyazawa A, Fujiyoshi Y, and Unwin N (2003) Structure and gating mechanism of the acetylcholine receptor pore. *Nature (Lond)* **423:**949–955.

Mukhtasimova N, Free C, and Sine SM (2005) Initial coupling of binding to gating mediated by conserved residues in the muscle nicotinic receptor. *J Gen Physiol* **126:**23–39.

Newell JG, McDevitt RA, and Czajkowski C (2004) Mutation of glutamate 155 of the GABAA receptor beta2 subunit produces a spontaneously open channel: a trigger for channel activation. *J Neurosci* **24:**11226–11235.

Papke RL and Heinemann SF (1994) Partial agonist properties of cytisine on neuronal nicotinic receptors containing the β2 subunit. *Mol Pharmacol* **45:**142–149.

Papke RL and Porter Papke JK (2002) Comparative pharmacology of rat and human alpha7 nAChR conducted with net charge analysis. *Br J Pharmacol* **137:**49–61.

Rajendra S, Lynch JW, Pierce KD, French CR, Barry PH, and Schofield PR (1995) Mutation of an arginine residue in the human glycine receptor transforms beta-alanine and taurine from agonists into competitive antagonists. *Neuron* **14:**169–175.

Sala F, Mulet J, Sala S, Gerber S, and Criado M (2005) Charged amino acids of the N-terminal domain are involved in coupling binding and gating in α7 nicotinic receptors. *J Biol Chem* **280:**6642–6647.

Sala F, Mulet J, Valor LM, Criado M, and Sala S (2002) Effects of benzothiazepines on human neuronal nicotinic receptors expressed in *Xenopus* oocytes. *Br J Pharmacol* **136:**183–192.

Schofield CM, Jenkins A, and Harrison NL (2003) A highly conserved aspartic acid residue in the signature disulfide loop of the α1 subunit is a determinant of gating in the glycine receptor. *J Biol Chem* **278:**34079–34083.

Sigel E, Buhr A, and Baur R (1999) Role of the conserved lysine residue in the middle of the predicted extracellular loop between m2 and m3 in the GABA(A) receptor. *J Neurochem* **73:**1758–1764.

Sine SM, Quiram P, Papanikolaou F, Kreienkamp HJ, and Taylor P (1994) Conserved tyrosines in the α subunit of the nicotinic acetylcholine receptor stabilize quaternary ammonium groups of agonists and curariform antagonists. *J Biol Chem* **269:**8808–8816.

Sine SM, Shen XM, Wang HL, Ohno K, Lee WY, Tsujino A, Brengmann J, Bren N, Vajsar J, and Engel AG (2002) Naturally occurring mutations at the acetylcholine receptor binding site independently alter ACh binding and channel gating. *J Gen Physiol* **120:**483–496.

Unwin N (2005) Refined structure of the nicotinic acetylcholine receptor at 4A resolution. *J Mol Biol* **346:**967–989.

Address correspondence to: Dr. Francisco Sala, Instituto de Neurociencias de Alicante, Universidad Miguel Hernández-CSIC, Apartado 18, 03550-Sant Joan d'Alacant, Alicante, Spain. E-mail: fsala@umh.es